Supplementary Information

Organic nanoelectronics inside us: charge transport and localization in RNA could orchestrate ribosome operation

Andrey Sosorev[1,2]* and Oleg Kharlanov[2]

[1] *Shemyakin-Ovchinnikov Institute of bioorganic chemistry of the Russian Academy of Sciences, Ulitsa Miklukho-Maklaya, 16/10, Moscow, GSP-7, 117997, Russia*

[2] *Faculty of Physics, Lomonosov Moscow State University, Leninskie Gory 1/2, Moscow 119991, Russia*

*e-mail: sosorev@physics.msu.ru

S1. Hole transfer integrals and transfer rates

Table S1 Hole transfer integrals (absolute values) between various sites (only those exceeding 1 meV are presented) calculated for molecular mechanics (MM) and DFT-optimized geometries of the nucleobases.

Site pairs *a–b*	Site types	$\lvert J_{ab}\rvert$, eV		Site pairs *a–b*	Site types	$\lvert J_{ab}\rvert$, eV		Site pairs *a–b*	Site types	$\lvert J_{ab}\rvert$, eV		Site pairs *a–b*	Site types	$\lvert J_{ab}\rvert$, eV	
		MM geom.	DFT geom.			MM geom.	DFT geom.			MM geom.	DFT geom.			MM geom.	DFT geom.
1–2	G–C	0.156	0.170	10–24	G–G	0.005	0.006	26–44	A–G	0.010	0.007	50–64	U–A	0.015	0.021
1–71	G–G	0.007	0.008	10–25	G–C	0.023	0.030	27–28	G–G	0.007	0.001	50–65	U–G	0.027	0.022
2–3	C–G	0.012	0.008	10–26	G–A	0.111	0.117	27–43	G–C	0.015	0.002	51–52	U–G	0.002	0.002
3–4	G–C	0.136	0.153	10–44	G–G	0.012	0.019	28–29	G–G	0.001	0.015	51–63	U–G	0.008	0.010
3–69	G–G	0.001	0.002	11–12	C–U	0.045	0.051	28–42	G–C	0.023	0.034	51–64	U–A	0.004	0.010
3–70	G–C	0.021	0.031	11–23	C–A	0.003	0.002	28–43	G–C	0.049	0.024	52–53	G–G	0.079	0.094
3–71	G–G	0.086	0.081	11–24	C–G	0.011	0.006	29–30	G–G	0.069	0.076	52–63	G–G	0.052	0.029
4–5	C–G	0.004	0.004	11–25	C–C	0.017	0.012	29–41	G–C	0.004	0.001	53–54	G–U	0.191	0.204
4–69	C–G	0.002	0.001	12–13	U–C	0.036	0.028	29–42	G–C	0.055	0.037	53–58	G–A	0.003	0.002
4–70	C–C	0.059	0.041	12–23	U–A	0.026	0.016	30–31	G–A	0.005	0.013	53–61	G–C	0.024	0.020
5–6	G–G	0.071	0.085	12–24	U–G	0.013	0.006	30–40	G–C	0.020	0.021	53–62	G–C	0.018	0.008
5–68	G–C	0.023	0.031	13–14	C–A	0.019	0.016	30–41	G–C	0.016	0.006	54–55	U–U	0.105	0.097
5–69	G–G	0.091	0.074	13–22	C–G	0.014	0.014	31–32	A–U	0.080	0.094	54–58	U–A	0.006	0.009
6–7	G–A	0.033	0.040	13–23	C–A	0.030	0.006	31–38	A–A	0.014	0.014	54–61	U–C	0.007	0.004
6–67	G–C	0.017	0.024	14–15	A–G	0.067	0.073	31–39	A–U	0.013	0.002	55–56	U–C	0.003	0.005
6–68	G–C	0.058	0.041	14–21	A–A	0.003	0.003	31–40	A–C	0.071	0.045	55–57	U–G	0.064	0.060
7–49	A–C	0.044	0.092	14–22	A–G	0.130	0.137	32–33	U–U	0.068	0.101	55–58	U–A	0.002	0.002
7–65	A–G	0.002	0.001	15–21	G–A	0.015	0.022	32–38	U–A	0.001	0.013	56–57	C–G	0.039	0.038
7–66	A–U	0.017	0.021	15–48	G–C	0.008	0.010	33–35	U–A	0.040	0.047	58–60	A–U	0.001	0.002
7–67	A–C	0.060	0.029	15–59	G–U	0.001	0.005	33–36	U–A	0.002	0.005	58–61	A–C	0.139	0.100
8–13	U–C	0.069	0.082	18–55	G–U	0.006	0.007	34–35	G–A	0.014	0.004	59–60	U–U	0.102	0.080
8–14	U–A	0.005	0.008	18–57	G–G	0.049	0.060	35–36	A–A	0.090	0.113	60–61	U–C	0.003	0.003
8–15	U–G	0.003	0.019	18–58	G–A	0.011	0.024	36–37	A–A	0.134	0.145	61–62	C–C	0.001	0.001
8–21	U–A	0.001	0.001	19–56	G–C	0.002	0.001	37–38	A–A	0.071	0.076	62–63	C–G	0.006	0.001
8–22	U–G	0.003	0.002	19–57	G–G	0.081	0.101	38–39	A–U	0.104	0.119	63–64	G–A	0.040	0.025
8–46	U–G	0.002	0.003	21–22	A–G	0.022	0.020	39–40	U–C	0.012	0.025	64–65	A–G	0.001	0.026
8–48	U–C	0.031	0.047	21–46	A–G	0.035	0.025	40–41	C–C	0.016	0.019	66–67	U–C	0.017	0.009
9–11	A–C	0.004	0.001	21–48	A–C	0.020	0.029	41–42	C–C	0.018	0.002	67–68	C–C	0.049	0.056
9–22	A–G	0.043	0.038	22–23	G–A	0.058	0.048	42–43	C–C	0.003	0.026	68–69	C – G	0.030	0.007
9–23	A–A	0.019	0.041	22–46	G–G	0.007	0.010	48–59	C–U	0.079	0.024	69–70	G – C	0.039	0.090
9–24	A–G	0.004	0.005	23–24	A–G	0.120	0.125	49–50	C–U	0.013	0.012	70–71	C – G	0.028	0.006
9–44	A–G	0.055	0.034	24–25	G–C	0.011	0.001	49–65	C–G	0.014	0.021				
9–46	A–G	0.004	0.014	25–26	C–A	0.029	0.032	49–66	C–U	0.020	0.017				
10–11	G–C	0.033	0.040	26–27	A–G	0.022	0.054	50–51	U–U	0.095	0.087				

Table S2. HOMO energies for various tRNA bases (sites) that participate in charge migration.

base	E_{HOMO}, eV	base	E_{HOMO}, eV	base	E_{HOMO}, eV	base	E_{HOMO}, eV
1	-5.227	21	-5.723	39	-6.506	59	-6.487
2	-5.717	22	-5.263	40	-5.758	60	-6.533
3	-5.241	23	-5.709	41	-5.736	61	-5.709
4	-5.761	24	-5.246	42	-5.733	62	-5.744
5	-5.246	25	-5.728	43	-5.78	63	-5.208
6	-5.255	26	-5.752	44	-5.241	64	-5.687
7	-5.717	27	-5.206	46	-5.276	65	-5.216
8	-6.509	28	-5.249	48	-5.752	66	-6.46
9	-5.731	29	-5.26	49	-5.731	67	-5.788
10	-5.165	30	-5.249	50	-6.514	68	-5.752
11	-5.747	31	-5.709	51	-6.476	69	-5.244
12	-6.46	32	-6.501	52	-5.252	70	-5.744
13	-5.763	33	-6.455	53	-5.225	71	-5.233
14	-5.717	34	-5.184	54	-6.46		
15	-5.255	35	-5.769	55	-6.463		
18	-5.206	36	-5.801	56	-5.793		
19	-5.265	37	-5.695	57	-5.178		
21	-5.723	38	-5.717	58	-5.706		

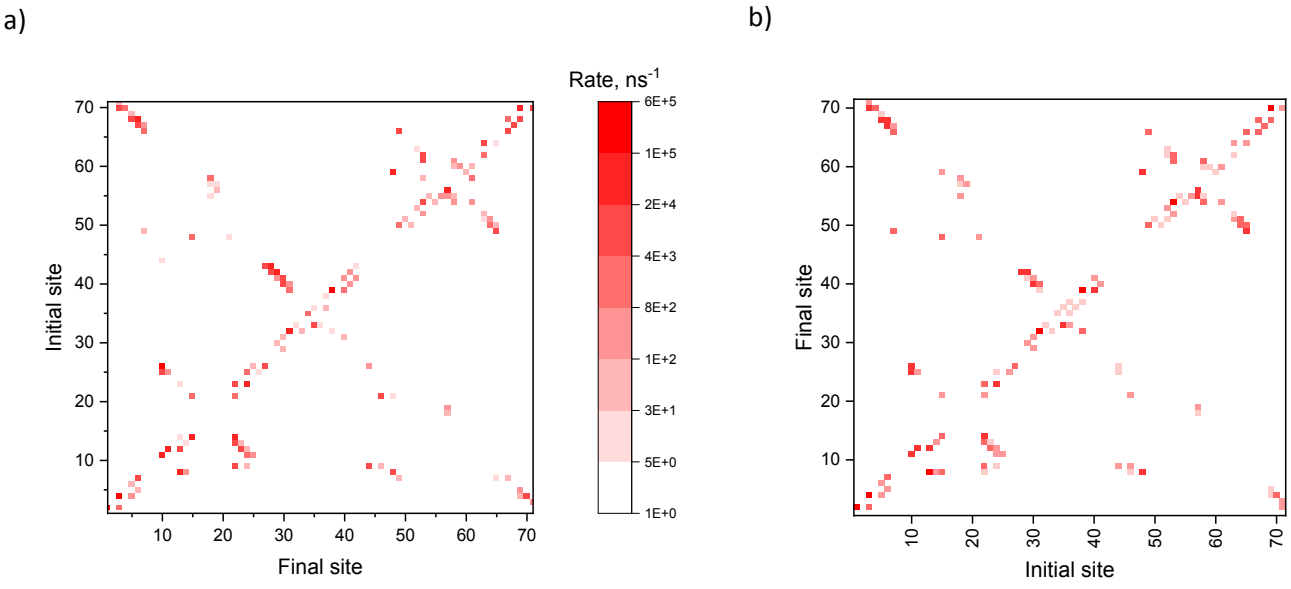

Fig. S1 Hole transfer rates k_{ab} between various sites of $tRNA^{Phe}$, in ns^{-1}, for MM- (a) and DFT-optimized (b) geometries of nucleobases.

S2. Dynamics of charge localization

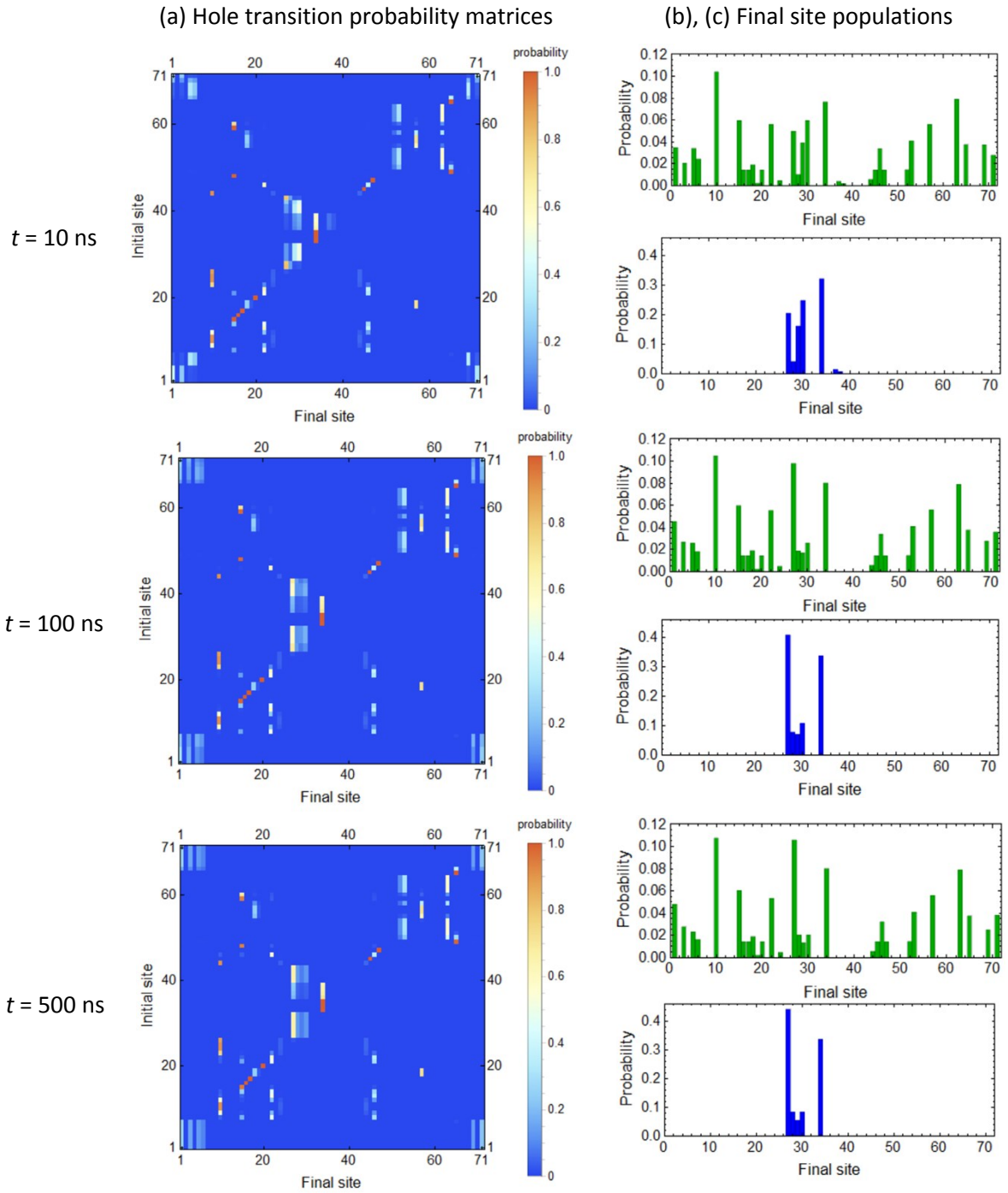

Fig. S2 Dynamics of hole localization pattern in tRNA^{Phe}: (a) transition probability matrices and (b), (c) site (nucleobase) populations at different moments of time. Green and blue bars in panels (b), (c) demonstrate populations for a hole starting from an arbitrary site of the whole tRNA and from an arbitrary site within the anticodon stem-loop, respectively

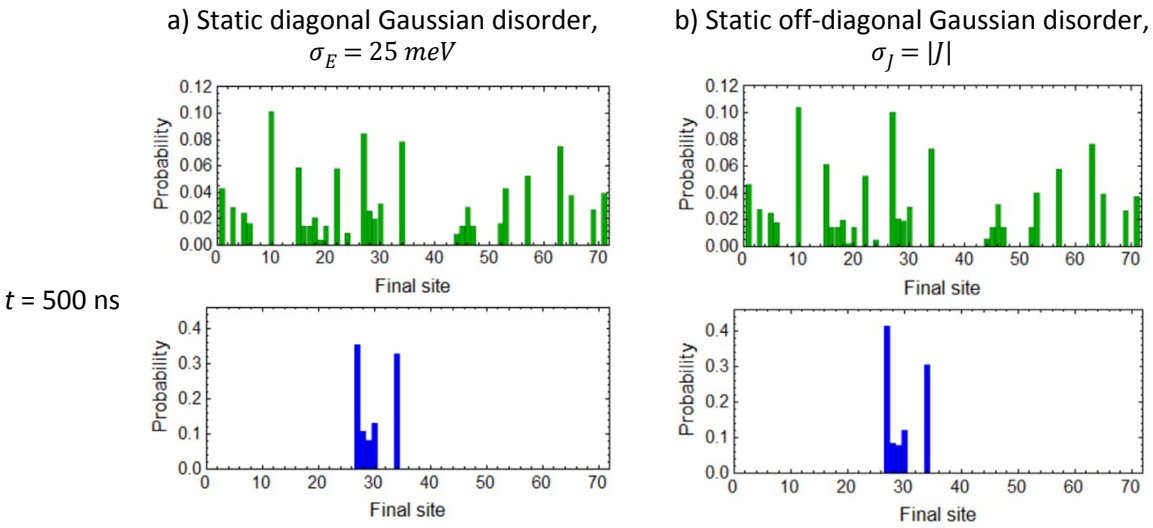

Fig. S3 Effect of Gaussian static diagonal (a) and off-diagonal (b) disorder on hole localization in tRNA^{Phe}. Green and blue bars demonstrate populations for a hole starting from an arbitrary site of the whole tRNA and from an arbitrary site within the anticodon stem-loop, respectively

S3. Electrostatic potential of nucleobases

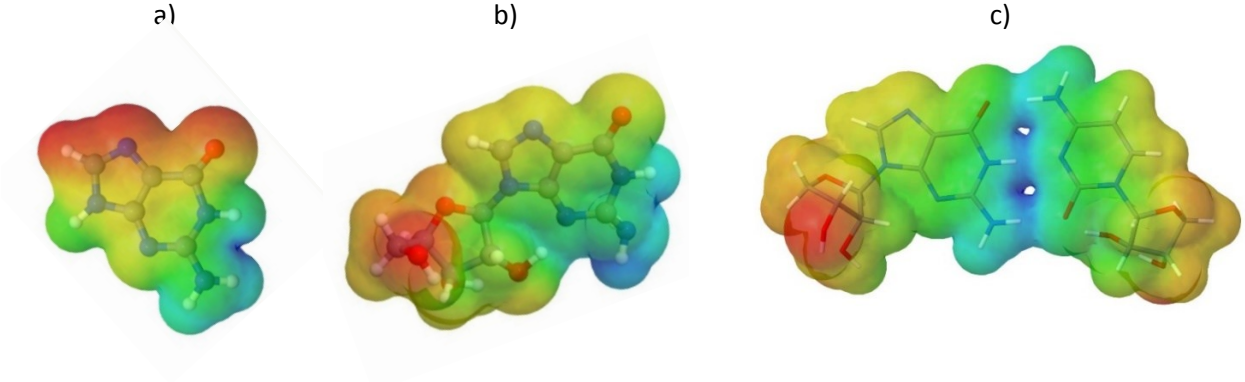

Fig. S4 Electrostatic potential of guanine (a), guanosine (b) and G-C pair (c). Red color stands for negative electrostatic potential, and blue color stands for positive electrostatic potential

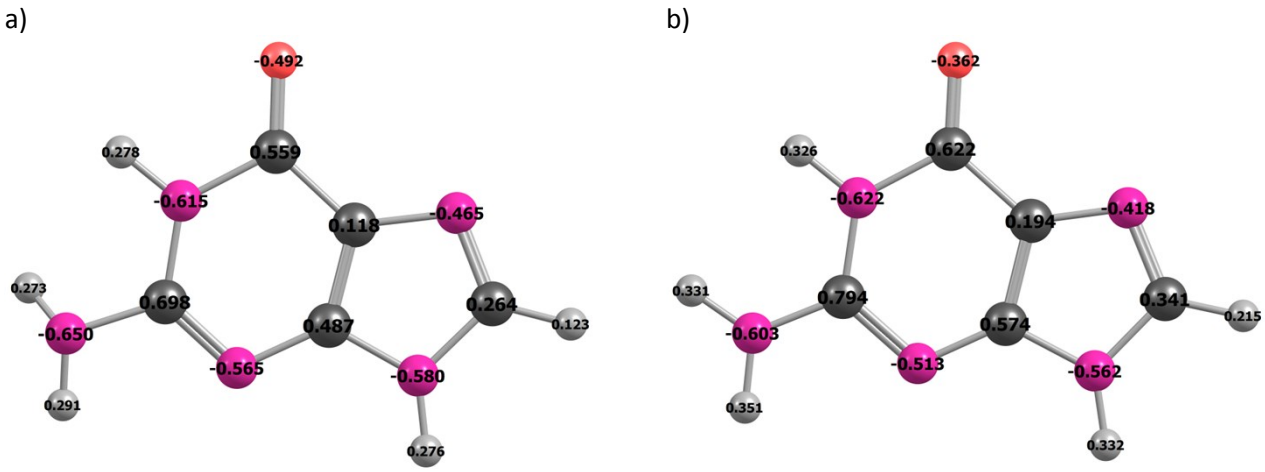

Fig. S5 Mulliken charges in the neutral (a) and cation (b) states of the guanine nucleobase

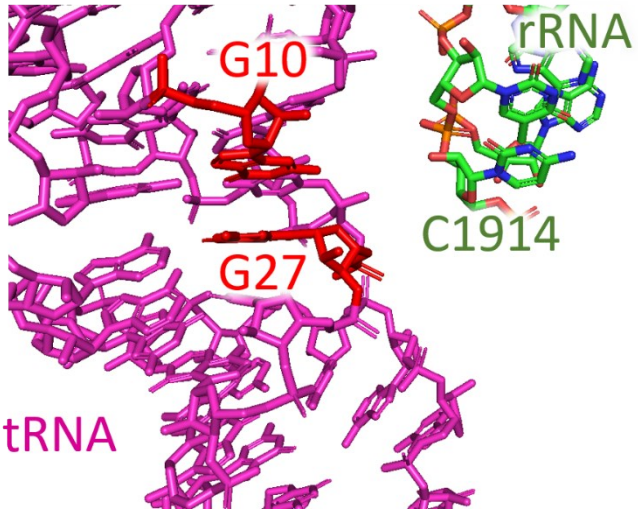

Fig. S6 rRNA nucleotides in the vicinity of G27 and G10.

S4. Molecular dynamics

The nanosecond-scale MD simulations have been carried out by us mainly to qualitatively test robustness of our conclusions on the hole localization against thermal motion of the tRNA molecule. Apart from that, even though tRNA conformational dynamics are typically characterized with longer timescales, we wanted to check if there possibly are any short-time effects of the localized charge on the tRNA conformations within the simplest setup (without the neighboring EF–Tu factor and the ribosome).

MD simulations included those of a single $tRNA^{Phe}$ molecule neutralized with sodium counterions in explicit water solvent, as well as those dealing with a $tRNA^{Phe}$ hosting a hole at G27 (and the number of counterions decreased by one). As we indicated in the Methods section of the paper, a standard AMBER RNA force field ff99 + bsc0 + χOL3 was used for tRNA, while water was described by the TIP3P model and processed using the SHAKE algorithm. The whole system was placed into a periodic truncated octahedral box, keeping the tRNA no less than 8 Å from the walls.

MD simulations of the 'neutral' and the 'charged' tRNAs were performed independently: initial energy optimization was followed by heating from T = 0 to T = 300 K and equilibration, prior to making a production MD. Quite conventionally, the energy was optimized first by adjusting the geometry of the solvent and the counterions, with restrained tRNA atoms, and only after that the system as a whole was optimized. Further preparation of the system included a 0.25 ns NVT heating to room temperature, with the temperature controlled via Langevin dynamics, and another 0.5 ns of an NpT simulation at the atmospheric pressure. After all these steps, we have simulated 5 MD trajectories, each of them 2 ns long (i.e., the total simulation time is 10 ns), for both the 'charged' and the 'neutral' molecule.

During post-processing, we sampled the trajectories obtained to extract the dynamics of the Φ angle between nucleotides No. 72, 55, 24 controlling the tRNA kinking (see Fig. S7), as well as to sample the geometries of neighboring nucleobases. The nucleobase pairs were then processed using the same DFT-based methodology as in the case of the optimized geometry, giving the transfer integrals and the on-site energies as an output (Table S3). As one can see from Fig. S7, within the timespan processed, the effect of the positive charge localized on the G27 nucleotide cannot be separated from the thermal noise, so considerably longer and time-consuming simulations are clearly necessary to draw any definitive conclusions on its physical and biological relevance.

a)

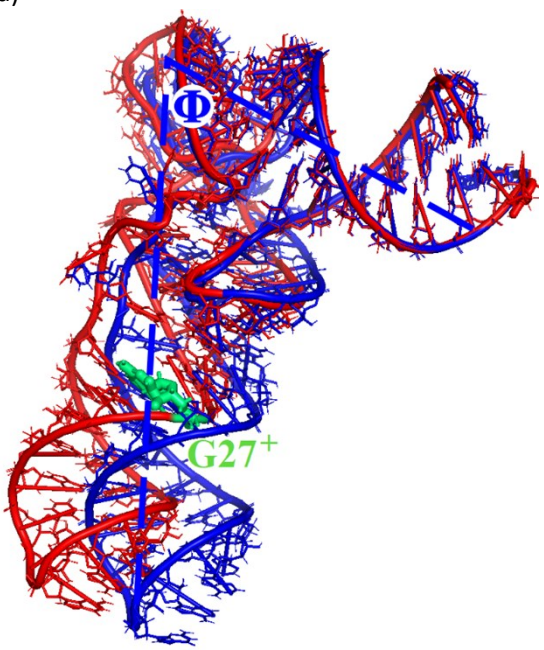

b)

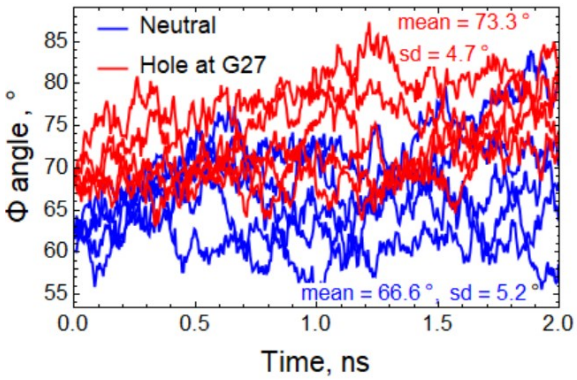

Fig. S7 A short-timespan MD simulation of tRNA in explicit solvent with sodium counterions: (a) average tRNA geometry sampled from 10 ns of total simulation time and (b) time dynamics of the Φ angle between the acceptor and anticodon stems. The geometries of the original, 'neutral' tRNA and the 'charged' tRNA with a hole localized at its G27 nucleotide are shown in blue and red, respectively; the G27 nucleotide itself is shown in green in panel (a).

Table S3. Variations of charge transfer integrals (in meV) with time from MD simulation.

Time, ps	0	43	86	129	172	215	258	301	344	387	430	473	516	558
A9-G44	107	123	143	51	3	18	23	24	15	118	94	58	28	68
A9 - G22	71	27	34	74	16	21	61	14	44	42	10	26	14	36
A9 - C11	3	3	2	1	12	1	3	0	2	3	8	4	4	5
U8 - C48	12	4	31	26	33	17	15	17	10	19	8	3	4	5
U8 - G46	2	1	2	2	1	0	1	1	1	0	1	1	1	1
U8 - G15	18	17	9	36	7	20	21	2	17	2	8	11	36	14
U8 - C13	103	87	96	57	54	41	114	49	38	154	74	88	172	51
A7 - C67	24	110	90	68	32	86	1	15	59	94	4	102	2	73
G69 - C70	111	70	112	106	41	121	208	116	115	91	0	86	113	128
U66 - C67	2	12	7	18	39	0	4	26	26	5	34	3	4	20
G63 - A64	15	70	66	42	73	92	23	48	7	24	74	66	35	12
U60 - C61	1	1	1	4	4	1	1	1	0	0	1	1	0	0
A58 - C61	240	75	138	209	200	91	42	64	161	80	155	61	66	32
U55 - G57	50	23	65	13	103	31	44	57	44	35	35	47	51	48
U54 - A58	29	9	4	6	10	12	11	39	5	29	11	18	6	27
U54 - U55	95	125	113	147	122	77	93	77	143	4	65	73	152	111
G52 - G63	28	19	5	40	40	57	16	7	21	18	8	8	15	18
U51 - G63	12	7	8	8	3	13	4	10	14	8	6	8	2	1
U50 - A64	19	18	6	15	26	4	13	11	17	25	8	11	14	15
G5 - G69	13	87	36	51	105	109	12	101	40	46	5	33	79	28
C40 - C41	34	27	35	4	8	21	17	62	104	39	13	33	59	44

C4 - C70	32	53	10	49	55	69	38	52	17	35	7	6	4	34
C4 - G69	22	22	16	2	6	18	10	12	8	17	5	30	23	15
A38 - U39	87	22	53	67	124	13	53	95	143	146	53	16	12	26
A37 - A38	45	67	112	34	22	31	55	41	36	55	49	9	11	17
A36 - A37	38	91	98	71	71	3	50	57	156	0	11	111	118	86
G34 - A35	65	66	105	5	25	99	6	45	27	53	146	68	23	38
U33 - A35	28	78	12	20	26	46	42	53	36	36	61	55	21	35
U32 - U33	21	17	69	125	59	177	44	153	186	98	117	192	70	26
A31 - C40	52	57	85	35	41	30	43	51	61	41	128	11	68	86
A31 - A38	5	16	8	26	1	7	76	27	20	20	34	3	16	8
G30 - C41	90	78	128	14	56	111	149	90	30	27	22	36	23	131
G30 - A 31	47	83	83	35	21	37	25	19	18	12	13	44	9	14
G3 - G71	29	89	13	28	61	88	37	58	63	21	98	86	109	115
G3 - G69	1	1	1	0	0	0	3	1	5	2	22	16	11	2
G3 - C4	57	66	124	41	73	119	129	114	62	79	48	30	139	102
G29 - C41	4	13	28	24	29	14	31	2	37	8	23	15	24	10
G28 - G29	58	25	10	59	36	2	22	63	82	10	2	49	53	80
G27 - G28	39	89	6	7	33	62	34	95	27	8	39	6	89	41
A26 - G27	33	80	129	86	129	71	8	185	89	86	26	118	146	115
C25 - A26	47	24	4	28	39	50	2	3	29	16	7	24	14	7
G22 - A23	56	50	104	21	5	76	0	85	105	63	60	68	25	95
A21 - G22	57	23	55	122	34	62	79	65	97	86	32	56	32	29
G19 - G57	79	62	53	116	134	41	87	58	71	47	92	60	51	95
G18 - G57	45	27	85	61	47	78	107	109	33	36	50	54	13	42
G18 - U55	9	17	17	3	24	9	1	15	8	13	12	15	31	22
G15 - C48	13	3	31	33	6	7	48	8	31	8	9	18	2	7
G15 - A21	21	48	41	19	23	34	5	1	6	2	9	12	5	39
C13 - G22	19	14	19	11	22	23	17	19	15	27	5	12	1	32
C13 - A14	31	31	15	40	31	46	16	25	51	27	43	22	63	29
U12 - G24	9	48	1	16	6	12	54	21	7	0	3	5	13	13
C11 - C25	74	75	17	9	2	7	30	12	54	4	15	14	21	12
C11 - A23	0	1	0	1	4	0	1	0	2	4	2	1	5	3
C11 - U12	69	9	32	19	35	24	114	51	106	61	24	10	68	25
G10 -G44	7	13	3	5	0	0	0	0	4	6	0	2	1	12
G10 - A26	4	24	45	24	18	65	5	108	82	3	13	63	62	70
G10 - G24	1	7	7	11	2	8	1	1	2	4	3	4	6	4
G10 - C11	90	144	89	60	14	22	30	115	34	6	26	39	60	15

S5. Pathway from 4Fe4S to tRNA

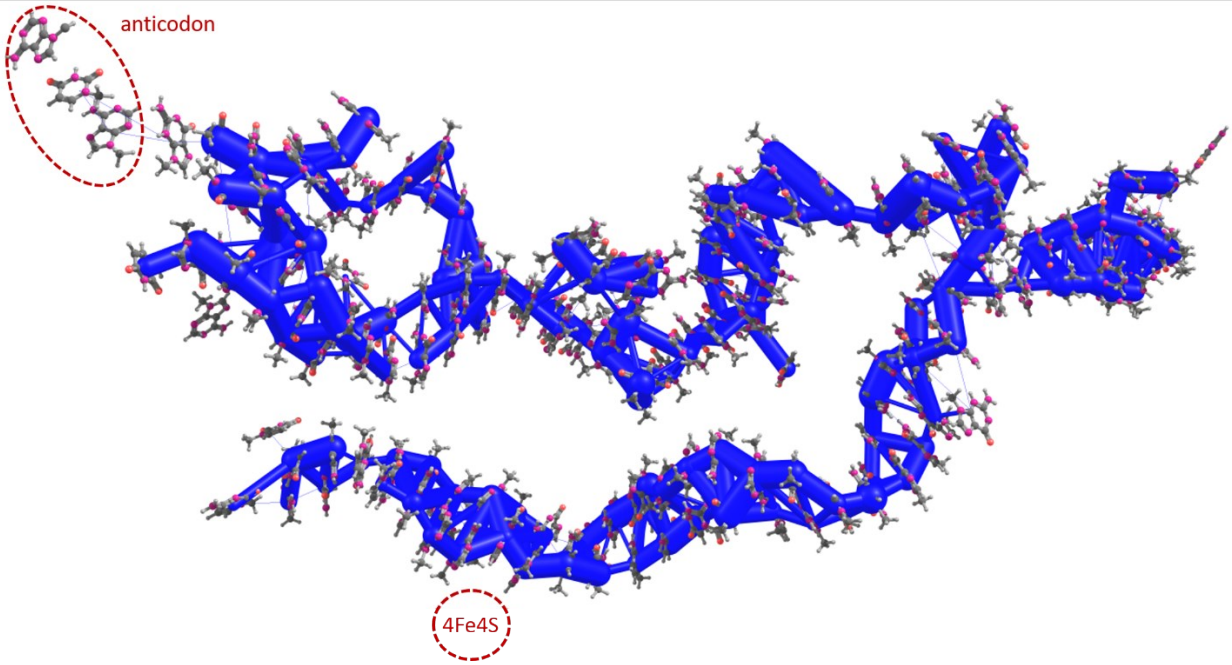

Fig. S8 Hole transfer integrals *J* within the pathway from 4Fe4S to tRNA. The thickness of the cylinders represents the magnitude of *J* in the logarithmic scale; the largest *J* amount to 160 meV, the smallest drawn are of the order of 10 meV.